J6.6 MESOSCALE MOISTURE TRANSPORT BY THE LOW-LEVEL JET DURING THE IHOP FIELD EXPERIMENT

Edward I. Tollerud[1], Fernando Caracena[1], Diana L. Bartels[1], Steven E. Koch[1], Brian D. Jamison[1,2], R. Michael Hardesty[3], Brandi. J. McCarty[4], W. Alan Brewer[3], Randall S. Collander[1,2], Steven Albers[1,2], Brent Shaw[5], Daniel L. Birkenheuer[1], and Christoph Kiemle[6]

[1]NOAA Research – Forecast Systems Laboratory, Boulder, CO
[2]Cooperative Institute for Research in the Atmosphere (CIRA), Fort Collins, CO
[3]NOAA Research – Environmental Technology Laboratory
[4]Cooperative Institute for Research in the Environmental Sciences, Boulder, CO
[5]Weathernews, Inc., Oklahoma City, OK
[6]German Aerospace Center (DLR), Oberpfaffenhofen, Germany

1. INTRODUCTION

Previous studies of the Low-Level Jet (LLJ) over the central Great Plains of the United States have been unable to determine the role that mesoscale circulations play in the transport of moisture. To address this issue, two aircraft missions during the International H_2O Experiment (IHOP) were designed to closely observe two separate well-developed LLJs over the Great Plains (primarily Oklahoma and Kansas) with multiple observation platforms. In addition to standard operational platforms (in particular, radiosondes and profilers) to provide the large-scale setting, dropsondes released from the aircraft at approximately 55 km intervals and a pair of onboard lidar instruments (HRDL for wind and DIAL for moisture) observed the moisture transport in the LLJ at greater resolution.

Two questions immediately present themselves: (1) Do focused observations at exceptionally high resolution provide details critical to our operational depiction of the LLJ; and (2) if they do, what is the physical nature of the circulations that are implied? A practical way of stating (1) is, do small-scale correlations between moisture and wind fluctuations within the LLJ significantly alter larger-scale estimates of LLJ moisture transport? To illustrate this possibility, we briefly compare the qualitative multi-scalar structure of the LLJ as revealed in point profiles and within vertical sections across the LLJ of wind, moisture, and resulting moisture transport as observed by multiple observation sets including radiosonde only, dropsondes, and simultaneous lidar measurements of moisture and wind. We then focus attention on the bulk properties and effects of scales of motion by computing layer-averaged fluxes through sections that bracket the LLJ. From these computations, we are able to compute Reynolds averages within the layers, from which we estimate the bulk effect of so-called ”prime-prime” terms, interpreted as integrated estimates of the contribution of small-scale (meso- to convective-scale) circulations to the overall transport. We then briefly describe modeling efforts that may eventually be able to describe mesoscale mechanisms that affect the LLJ moisture transport.

*Corresponding author address: Edward Tollerud, FSL/NOAA FS1, 325 Broadway, Boulder, Colorado, 80305.
email: edward.tollerud@noaa.gov

2. THE ROLE OF THE LLJ IN GREAT PLAINS MOISTURE TRANSPORT

Although the main purpose of IHOP was to characterize the structure of water vapor and water vapor transports, it was hoped that improved characterization of the transport of moisture, especially within the LLJ, could also provide important improvements in QPF. Along these lines, several studies have helped to establish the role of the LLJ as the major conveyor of low-level moisture from the Gulf of Mexico into the central United States (Stensrud 1996; Higgins et al. 1996). Overall, Higgins et al. (1997) estimate that the contribution of the LLJ to low-level moisture transport is almost 50% above average non-LLJ values. A major factor in the LLJ contribution to Central Plains precipitation is the relationship between the LLJ and

development of Mesoscale Convective Complexes, or MCCs (Maddox 1983; Augustine and Caracena 1994). Indeed, Fritsch et al. (1986) estimate that MCCs might be directly responsible for 1/3 or more of all warm season precipitation in the central United States. Anderson and Arritt (1998) describe the relationship between intense MCC development, synoptic setting, and the extreme precipitation that occurred in the flood-plagued northern Mississippi basin during the spring and summer of 1993.

Unfortunately, due to inadequate spatial or temporal resolution, the existing radiosonde network in the United States is not well suited to capture the LLJ. Climatological studies. using radiosondes have helped to clarify LLJ mechanisms (eg., Bonner 1968), but because they are often limited to a single observation within each LLJ sampled they cannot describe horizontal wind or thermodynamic gradients with precision. More recent studies employing the profiler network solve the time resolution issue (Mitchell et al. 1995; Anderson and Arritt 2001). However, these studies are affected by the fact that wind profilers often miss the very shallow LLJs that peak below the lowest observation gate (Whiteman et al. 1997; Daniel et al. 1999).

The use of dropsondes and lidar wind data in focused low-level jet studies have proven very useful (Banta et al. 2002; Ralph et al. 2005). However, to date there have been no studies that combine these measurements to describe the detailed horizontal mesoscale and sub-mesoscale structure of moisture transport within Central Plains LLJs.

In the numerical modeling arena, questions persist about the ability of existing operational models to adequately predict LLJ moisture transports. For instance, Anderson and Arritt (2001) conclude that NCEP-NCAR reanalysis fields significantly underestimate LLJ frequency. Limitations on model depiction of LLJ structure and evolution could be due to resolution problems or to model boundary layer physics that do not capture essential LLJ mechanisms.

3. THE 9 JUNE LLJ MISSION: FLIGHT STRATEGY AND SYNOPTIC SETTING

A summary of the IHOP field campaign, including its myriad of observation platforms, is provided in Weckwerth et al. (2004). For a detailed description of the 9 June LLJ aircraft mission, particularly its observation strategy, and snapshots of the structure of the LLJ on this morning, see Tollerud et al. (2004). The intent of this mission and another on June 3 was to deploy an array of observation platforms that cascaded from operational resolutions appropriate to describe the large-scale synoptic setting, to successively more detailed observation sets including dropsondes launched at roughly 55 km intervals from research aircraft down to sub-km-scale measurements by airborne moisture and wind-sensing instrumentation (respectively, the downward pointing Differential Absorption Lidar, or DIAL, and the High-Resolution Doppler Lidar, or HRDL, both on the DLR Falcon aircraft). Two dropsonde aircraft (the DLR Falcon and a Learjet) flew box patterns chosen to bracket the predicted location of the LLJ (Fig. 1). It was the original intent to have each aircraft complete the full rectangular circuit, refuel, and then repeat the circuit a second time. Instrumentation and aircraft constraints forced adaptations to the original plans, the principal change being the inability of the Falcon to fly the second circuit.

As the observations by the operational network in Figs. 1 and 2 show, the aircraft box on 9 June was well placed to bracket a strong LLJ that was in many ways a typical summertime example. At slightly lower altitudes than that shown on the figure (closer to the height of maximum winds), the core of the LLJ was more clearly oriented from the southwest side of the south aircraft leg to a point just west of the northeast corner of the box, near the eastern end of the north aircraft leg. Along the southern leg, the jet maximum was more spatially diffuse than it was along the north leg. At its western flank the jet layer itself is remarkably shallow, even as portrayed by the relatively coarse vertical coordinates of the model analysis (Fig. 2). The deeper layer of moisture transport east of the northern flight leg is primarily due to a deeper and moister boundary layer there

rather than to an increase in jet windspeed; at most levels the windspeed core is just west of the end of the flight track. Note the implied relationship between sloping terrain on jet location.

4. MULTISCALE OBSERVATIONS

In Fig. 3, three independently observed profiles of horizontal moisture flux are presented. All three show a shallow LLJ with a sharp transport maximum at about 1400 m above sea level (asl) with rapid gradients above and especially below the core. Clearly, at this location (near the eastern end of the southern leg) and time (near dawn, when the jet can be expected to be more nearly steady-state then it is later during heating-produced turbulent mixing), all three observation platforms provide remarkably similar pictures of LLJ moisture flux. In the case of radisonde observations, which are interpolated from neighboring launch sites to the location of the dropsonde profiles, the good agreement is likely due to the near-synoptic timing of the dropsonde, and to the possibility that the LLJ was fortuitously well captured by the radiosonde network. Radiosonde profiles at later off-synoptic times and at locations further from radiosonde launch sites exhibited significantly larger differences from collocated dropsonde and lidar profiles.

The close agreement between the dropsonde flux profile and that produced by the combination of DIAL and HRDL is strong confirmation that at a point both platforms appear to perform well. The performance of the DIAL and HRDL is especially satisfying, since IHOP was the first opportunity to use them in combination to compute fluxes. However, the figure also points out inter-platform observation differences with implications for later interpretation of flux computations. For example, the dropsondes have very much better vertical resolution, as shown by the spacing of the lidar points as compared to the nearly continuous dropsonde curves. Another difference is emphasized by the large magnitude of the observed flux transverse to the jet core (denoted as Dropsonde U in the figure) especially near the top of the jet core. Because the HRDL measured only one wind component (the along-jet, north-to-south component on the north and south legs) comparable lidar-based measurements of transport transverse to the jet were not available for comparison to dropsondes.

Mesoscale structures can reveal themselves either with vertical or horizontal features. Some variability in the vertical profile of moisture flux that could be mesoscale or smaller in origin is evident in Fig. 3. At a different point (near the jet core along the north leg) this variability is much more pronounced in both the wind and moisture fields (Fig. 4). Since these variations are all very nearly at a point, they could have originated from convection. There were in fact some shallow clouds in the region, but deep convection at this time in the morning and along a flight track selected to be hopefully free of convection is not likely and was not observed. Vertical wavelike features in the transport profile measured by dropsondes is also evident later in the day in the screen of meridional transport shown in Fig. 5. By this time the transport layer has significantly deepened with the onset of significant surface heating and consequent turbulent mixing.

Unfortunately, we do not have lidar data during the second circuit to determine if the more clearly apparent vertical features in the dropsonde section at this time are reflected in mesoscale or other horizontal variations. However, there is some suggestion of shallow vertical structures in the lidar fluxes observed during the early circuit (Fig. 6), though the scales cannot match those of the more finely resolved dropsonde measurements. In particular, there is an apparent dry layer at about 2000 m asll just at the eastern end of the flight leg (reflected in the transport section as a layer of reduced flux). Intriguingly, the dropsonde profile of moisture (Fig. 4) at this location also has a pronounced dry layer near this level. Complicating our interpretation of this feature is the fact that the u component of wind measured by the dropsonde shows a large spike in about the same layer. This greatly enhanced flux in the transverse direction is not reflected in the lidar-based computations.

The great advantage of the lidar flux measurements, of course, is the hugely

improved horizontal resolution they offer. In Fig 6, horizontal variations with dimensions of a few tens of km are evident (and confirmed by cospectral analyses not shown) throughout the LLJ layer. There are also some striking longer wavelike undulations of the top of the LLJ flux layer, particularly in the eastern half of the leg. We note that the dropsonde spacing cannot hope to resolve variations of tens of km in horizontal dimension, and can only marginally capture the longer waves. Unfortunately, the data available are not adequate to further explicate the physical nature of these variations.

Of particular interest to our study is the possibility that these small-scale horizontal features and vertical layers of moisture and wind could correlate strongly enough that operational observations that did not resolve them might significantly underestimate net transport within the LLJ. Fig. 7, which directly compares point measurements of lidar fluxes with dropsondes at a single height near the LLJ top, suggests that this might indeed be the case. At most (but not all) points along the leg the lidar fluxes are indeed larger. The comparison within the larger-scale undulations east of the section's central point are noteworthy in another respect; at the few points in these undulations where dropsonde measurements and lidar measurements were directly collocated, the two agree surprisingly well. It thus appears that the placement of dropsondes in this part of the leg was singularly unlucky, and unlikely to do justice to the transport. Of course, this is the essence of the resolution problem in a nutshell. We will attempt to assess the impact of resolution in a more integrated way in the next section.

5. BULK ESTIMATES OF MESOSCALE HORIZONTAL MOISTURE TRANSPORT

A more general issue than those taken up in previous sections, but one that is actually more fundamental, is this: can we demonstrate that small-scale circulations really do contribute in a significant way to total LLJ transports? One way to address this issue is to apply Reynolds averaging assumptions to estimate the magnitude of the fluxes that are not resolved by a particular set of observations. For horizontal moisture flux determined as the product of wind velocity (v) and specific humidity (q), we can pose the computation as:

$$\underline{v \times q} = \underline{v} \times \underline{q} + \underline{v' \times q'}$$

where the underbars indicate averages over a larger scale of interest and the primed terms are differences between the individual observations at smaller scales and the average itself. Stated in another way, underlying covariances due to small scale processes that are not resolved by the larger scale observations can contribute to the total observed flux measured at the larger scale. In the case of dropsonde observations, for instance, we might define the large scale as the average conditions along (say) the north leg of the flight box (something smaller than the effective resolution of the operational profiler network, perhaps), with the primed terms then being the differences between the individual dropsonde observations and the leg average. In this case, the covariances would be due to motions at horizontal scales resolved by observations that are ~55 km apart, and the large scale would be that resolved by averages at points separated by ~350 km (the length of the north leg of the flight box). We note that since the scale separation in this case is marginally adequate, the same set of computations using lidar observations that can be averaged to much smaller horizontal dimensions (not yet completed) would be more appropriate.

The results are shown in Fig. 8. Except for a layer near the top of the LLJ flux layer, the apparent contribution of dropsonde-resolved circulations to larger flight-box sized averages is small. We speculate that vertical undulations of the top of the LLJ flux layer similar to those discussed in the previous section could explain this result. Hopefully, computations using lidar observations will be able to confirm if these dropsonde results are meaningful.

The Reynolds averaging could alternately be applied to estimate the contributions by covariances in the vertical. For instance, the larger scale average could be defined by a deep layer (perhaps 200 m) and the primed variables could be the dropsonde

observations made every 15 m. Posed in this way, the results would address the questions raised about the apparent layered moisture and wind profiles in Fig. 4. The results of these computations (not shown) indicated no differences, and hence no net affect due to covariances between shallow layers of moisture and winds.

Another, more direct, way to get to an assessment of scales of fluxes is to simply compute within-layer leg averages of fluxes computed separately from lidar and from dropsondes. Fig. 9 shows the result, with net averages of lidar fluxes uniformly larger than those measured by dropsondes, except in the near surface layer, where the set of lidar measurements may not be complete enough to be representative. At the jet top, this result could be considered as confirmation of our interpretation of Fig. 8. However, within the rest (lower) part of the LLJ layer, another explanation would be required. We might speculate that in this layer the horizontal scale of the processes that contribute to the overall leg-averaged flux values are smaller than those at the layer top, and too small to be resolved by the dropsonde measurements.

6. THE SEARCH FOR MESOSCALE MECHANISMS: CONCLUSIONS AND FURTHER RESEARCH

As indicated by the analyses and observations presented in the two previous sections, there is evidence from IHOP that mesoscale processes might play a role in the horizontal transport of moisture by the LLJ. Further determination of the detailed physical nature of these processes, unfortunately, is limited by characteristics of our observations. Planned aircraft flights within the aircraft domain were not possible due to unforeseen flight restrictions after 9/11 and to logistic considerations during the experiment. In addition, the relocation of the center of gravity of field resources to the panhandle of Oklahoma away from numerous other permanent instrumentation resulted in fewer surface observations than hoped for within the LLJ aircraft domain. Another limiting factor was the unavailability of full wind measurements by the HRDL (only the wind component transverse to the aircraft flight path could be measured). As a result, we have not thus far been able to move beyond speculation concerning the actual small-scale physical processes that may have been contributing.

We have attempted to bridge these deficiencies by using observations as initialization for retrospective WRF model runs. Two fundamental modeling questions were addressed: how well could the LAPS-initiated 22-km WRF represent transports in the LLJ, and how great an impact would the inclusion of research observations (eg., dropsonde profiles along the flight box) have? To generally assess the former, we display initial WRF winds (small symbols) as the gridded backdrop to the observations (larger symbols) on Fig. 1. Clearly the model initial fields have captured the general structure of the LLJ. In Fig. 10 we present a comparison of the dropsonde-observed vertically-integrated transports along the north flight leg with comparable computations using WRF initialization fields (0-hr forecast; panel a) and 4-hr forecast fields (panel b). Although the initial WRF fields only slightly underestimate the magnitude of peak transport near the eastern end of the leg, it is clear that the analyses lack some sharpness in horizontal resolution. By 4 h the WRF model boundary layer physics have built a jet with strong features, but the forecast still underestimates the sharp horizontal gradient in transport. Planned analyses using 4 km MM5 simulations produced during the field phase may help resolve this problem, but the domain of the inner nest on this day only barely captured the north aircraft leg and could therefore be susceptible to boundary effects.

Concerning the impact of dropsonde data on the WRF forecasts, parallel initial analyses (not shown) with and without dropsonde data revealed no significant difference, and by 4 h into the WRF forecasts, differences in jet transport structure between runs was imperceptible. Although it is possible that this particular LLJ was so well captured by the operational observations that the dropsondes were superfluous, we believe it more likely that the analyses themselves are relatively insensitive to the existence of extra research data, at least as it is arrayed in this study. To

address this issue, it is likely that better vertical resolution in both analyses and models will be necessary before jets like these with such shallow features can be adequately represented. Until then, definitive clarification of the physical nature of mesoscale processes at work in these LLJ cases will have to rely on closer and more imaginative examination of the suite of dropsonde, lidar, and other observations from IHOP.

7. ACKNOWLEDGMENTS

We thank Chris Anderson and Susan Carsten for their reviews of this paper. Some of the work described here was supported by a grant from the United States Weather Research Program.

REFERENCES

Anderson, C.J, and R.W. Arrit, 1998: Mesoscale convective complexes and persistent elongated convective systems over the United States during 1992 and 1993. *Mon. Wea. Rev.*, **126**, 578-599.

Anderson, C.J., and R.W. Arrit, 2001: Representation of summertime low-level jets in the central United States by the NCEP-NCAR reanalysis. *J. Climate*, **14**,234-247.

Augustine, J. A. and F. Caracena, 1994: Lower tropospheric precursors to nocturnal MCS development over the central United States. *Wea. Forecasting*, **9**, 116-135.

Banta, R.M., R.K. Newsom, J.K. Lundquist, Y.L. Pichungina, R.L. Coulter, and L.J. Mahrt, 2002: Nocturnal low-level jet characteristics over Kansas during CASES-99. *Bound.-Layer Meteor.*, **105**, 221-252.

Daniel, C.J., R.W. Arrit, and C.J.Anderson, 1999: Accuracy of 404-MHz radar profilers for detection of low level jets over the central United States. *J. Appl. Meteor.*, **38**, 1391-1396.

Fritsch, J. M., R. J. Kane, and C. R. Chelius, 1986: The contribution of mesoscale convective weather systems to the warm-season precipitation in the United States. *J. Climate Appl. Meteor.*, **25**, 1333-1345.

Higgins, R.W., K.C. Mo, and S.D. Schubert, 1996: The moisture budget of the central United States in spring as evaluated in the NCEP/NCAR and the NASA/DAO reanalyses. *Mon. Wea. Rev.*, **124**, 939-963.

Higgins, R. W., Y. Yao, E. S. Yarosh, J. E. Janowiak, and K. C. Mo, 1997: Influence of the Great Plains low-level jet on summertime precipitation and moisture transport over the central United States. *J. Climate*, **10**, 481-507.

Maddox, R.A., 1983: Large-scale meteorological conditions associated with midlatitude mesoscale convective complexes. *Mon. Wea. Rev.*, **111**, 1475-1493.

Mitchell, M.J., R.W. Arritt, and K. Labas, 1995: A climatology of the warm season Great Plains low-level jet using wind profiler observations. *Wea. Forecasting,* **10**, 3028-3046.

Ralph, F.M., P.J. Neiman, and R. Rotunno, 2005: Dropsonde observations in low-level jets over the northeastern Pacific Ocean from CALJET-1998 and PACJET-2001: Mean vertical-profile and atmospheric-river characteristics. *Mon. Wea. Rev.*,**133**, 889-910.

Stensrud, D.J., 1996: Importance of low-level jets to climate: A review. *J. Climate*, **9**,1698-1711.

Tollerud, E.I., B.D. Jamison, F. Caracena, S.E. Koch, D.L. Bartels, R.M. Hardesty, B.J. McCarty, C. Kiemle, and G. Ehret, 2004: Multiscale analyses of moisture transport by the central plains low-level jet during IHOP. *20th Conf. on Weather Analysis and Forecasting*, Seattle, WA, Amer. Meteor. Soc., CD-ROM, P4.21.

Weckwerth, T. M., D. B. Parsons, S. E. Koch, J. A. Moore, M. A. Lemone, B. B. Demoz, C. Flamant, B. Geerts, J. Wang, and W. F. Feltz, 2004: An overview of the international H2O Project (IHOP 2002) and some preliminary highlights. *Bull. Amer. Meteor. Soc.*, **85**.

Whiteman, C.D., X. Bian, and S. Zhong, 1997:Low-level jet climatology from enhanced rawinsonde observations at a site in the southern Great Plains. *J. appl. Meteor.*, **36**, 1363-1376.

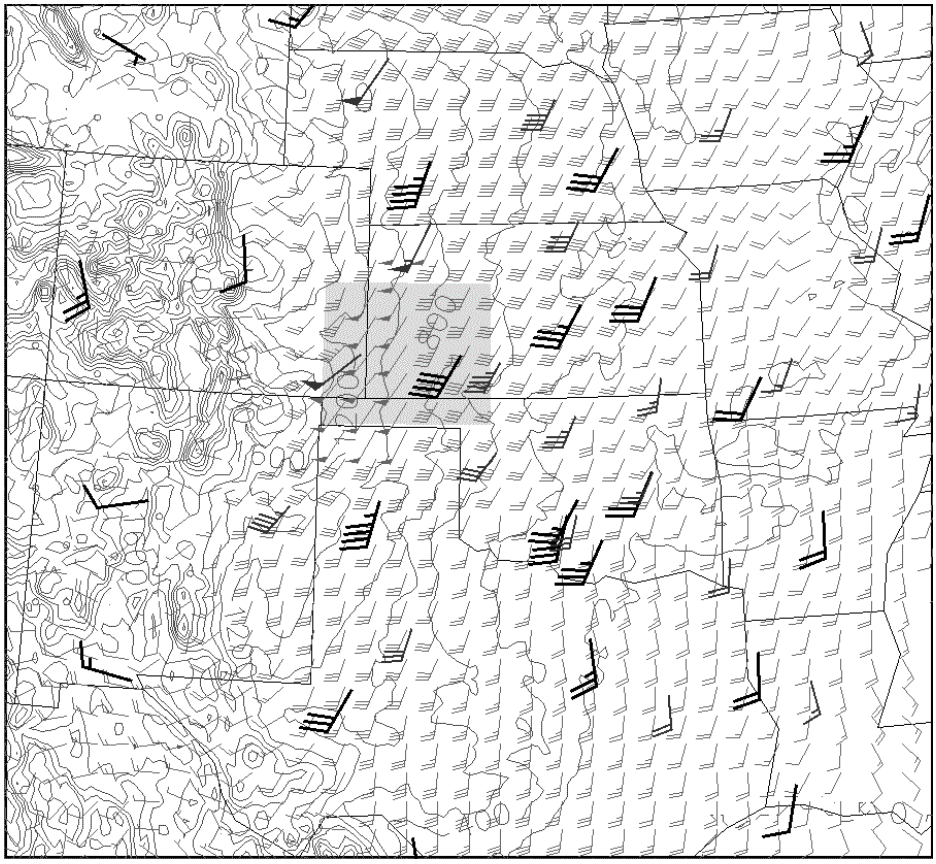

Fig. 1. Observed winds at 820 mb at 1200 UTC 9 June 2002. Largest wind barbs are observations at operational radiosonde observation sites, medium barbs are at profiler sites, and smallest gridded winds are at gridpoints of the WRF wind analysis at 1300 UTC. Terrain contours are displayed in increments of 400 m. The gray-shaded rectangular area denotes the aircraft flight box perimeter around which the two research aircraft flew during the 9 June LLJ mission.

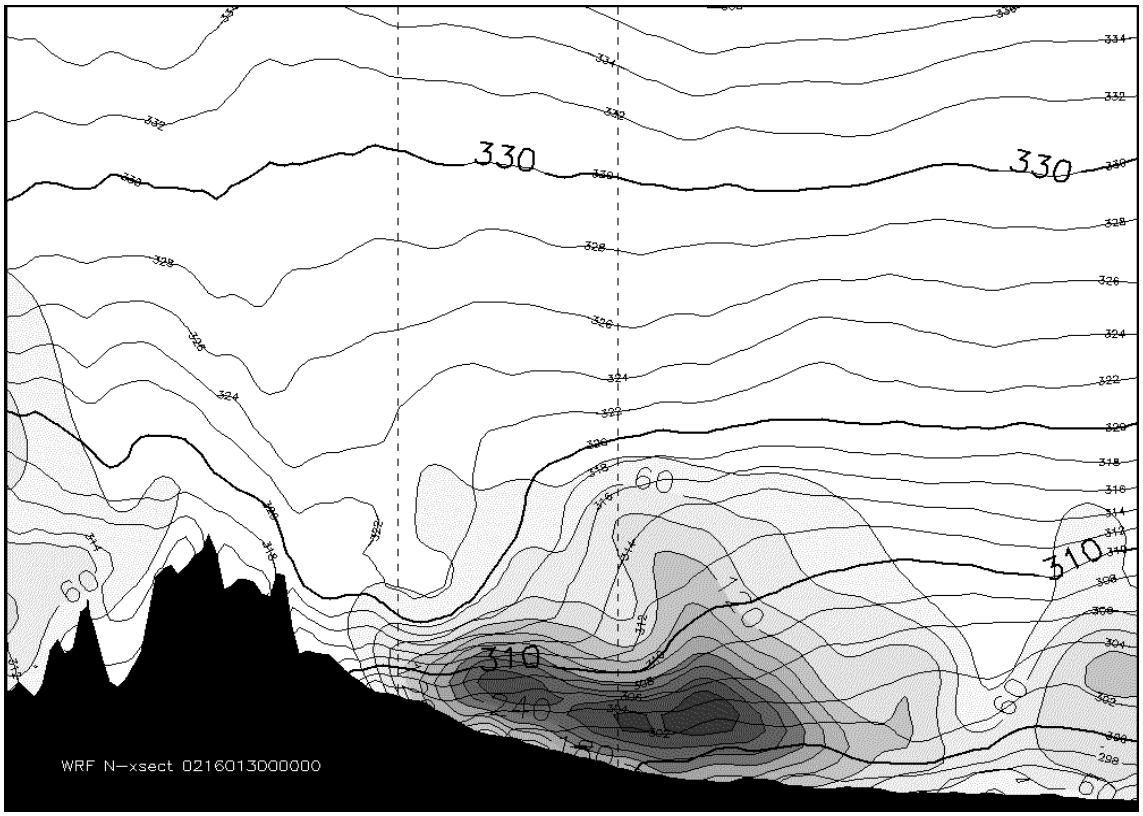

Fig. 2. Potential temperature (K) and northward meridional moisture flux (gkg^{-1} ms^{-1}) as analyzed in the 22 km WRF model analysis at 1300 UTC. Shown is a west-to-east vertical section that incorporates the northern leg of the rectangular flight track leg (see Fig. 1). Flight track end points are indicated by vertical dashed lines.

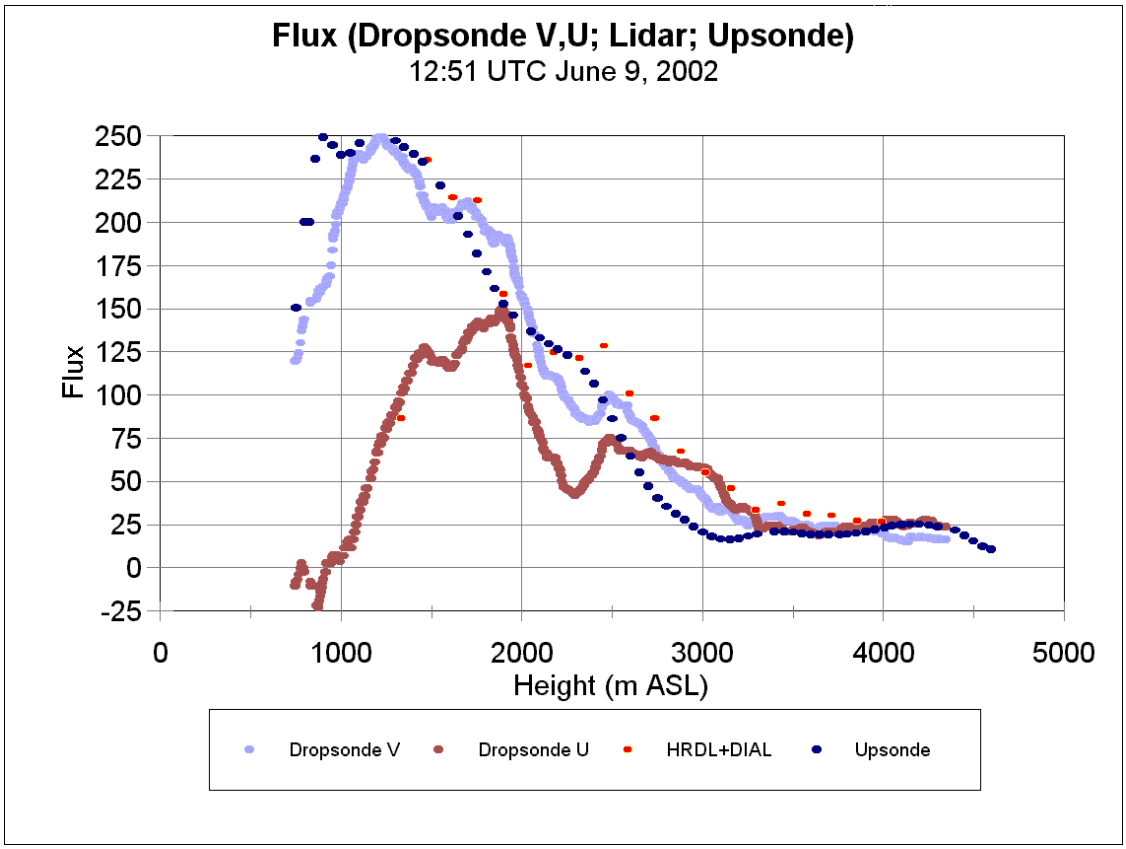

Fig. 3. Comparison of cross-track horizontal moisture transports(v x q) observed at 1251 UTC near the eastern end of the southern leg of the flight box on 9 June 2002. Units are gkg^{-1} ms^{-1}. Brown curve describes along-track transport observed by dropsondes but immeasurable by the DLR Falcon HRDL system.

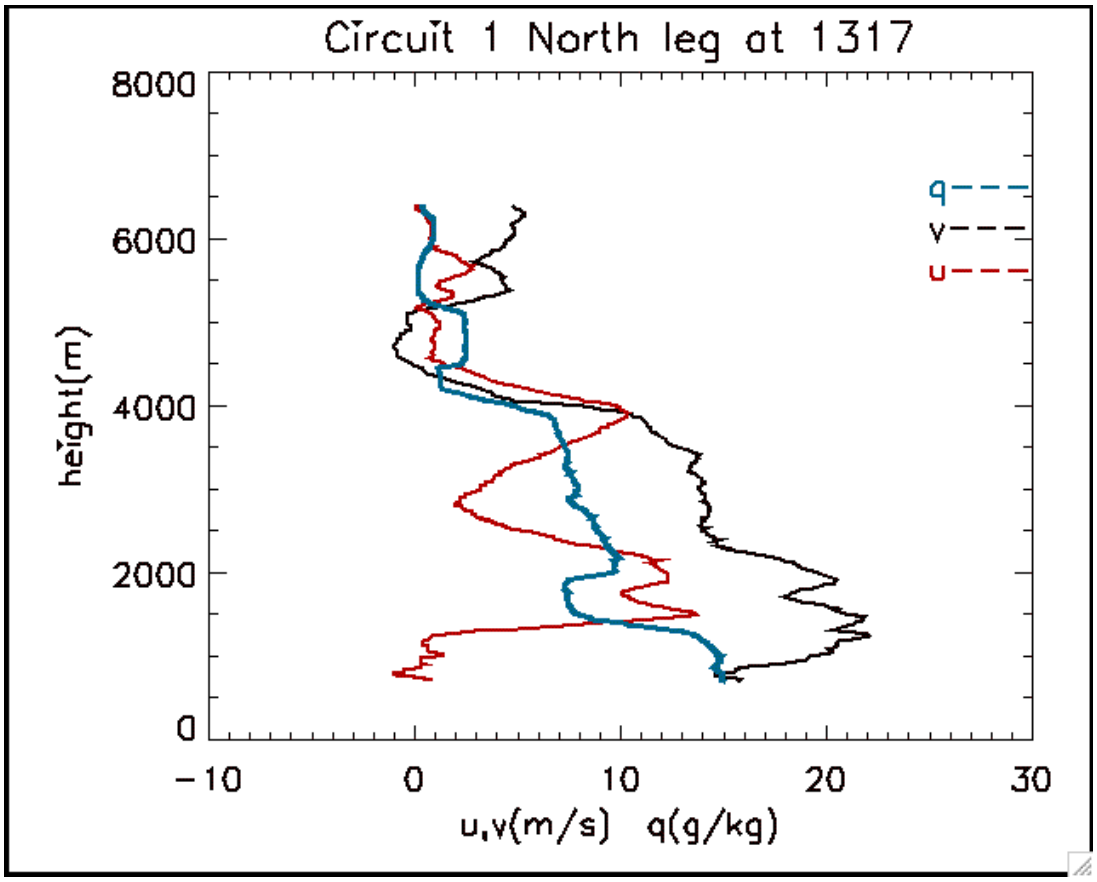

Fig. 4. Wind and moisture profiles observed by dropsonde launched from the Learjet at the core of the LLJ near the northeast corner of the flight domain on 9 June 2002. Heights are asl.

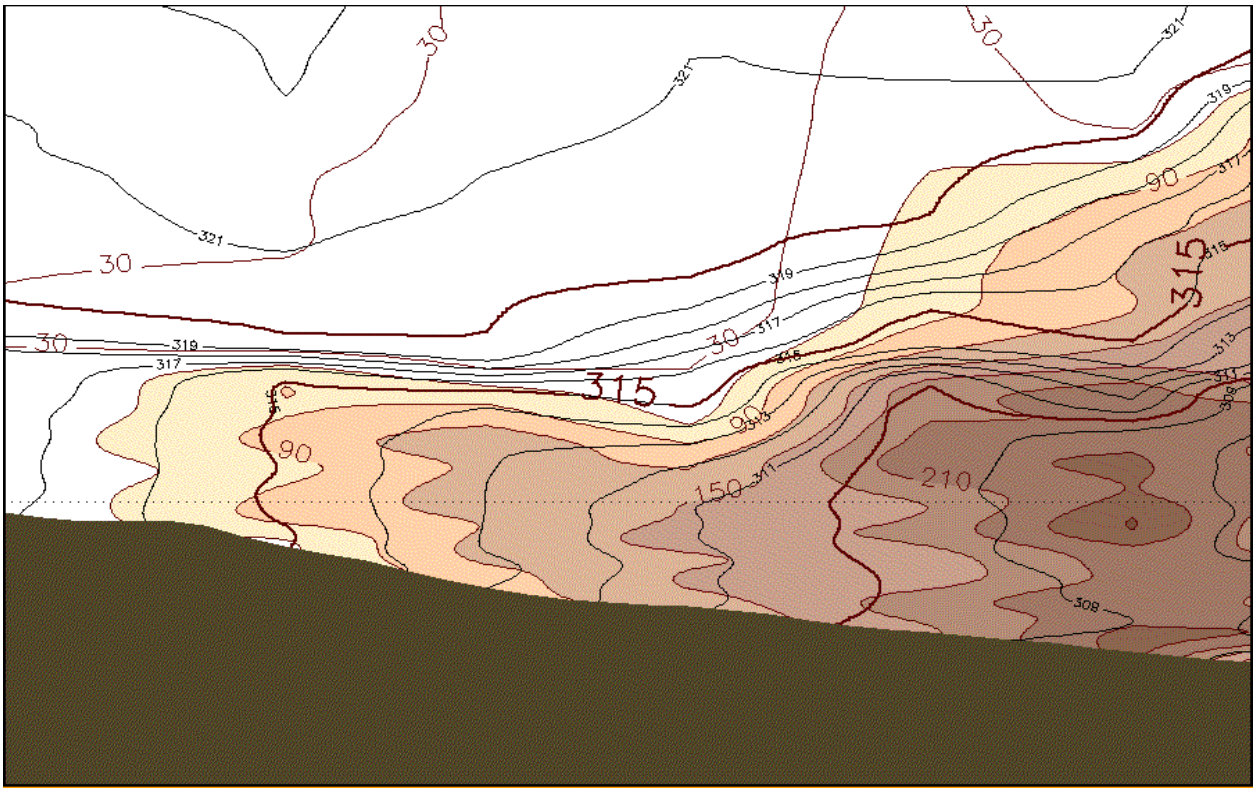

Fig 5. Potential temperature (heavy contours, intervals of 5 K) and northward meridional moisture flux (shaded, intervals of 30 gkg^{-1} ms^{-1}) through the northern flight leg during the second circuit of the Learjet (~ 1700 UTC 9 June 2002). Fluxes are computed and interpolated from dropsonde observations. See Figs. 1 and 2 for orientation and the text for instrumentation description.

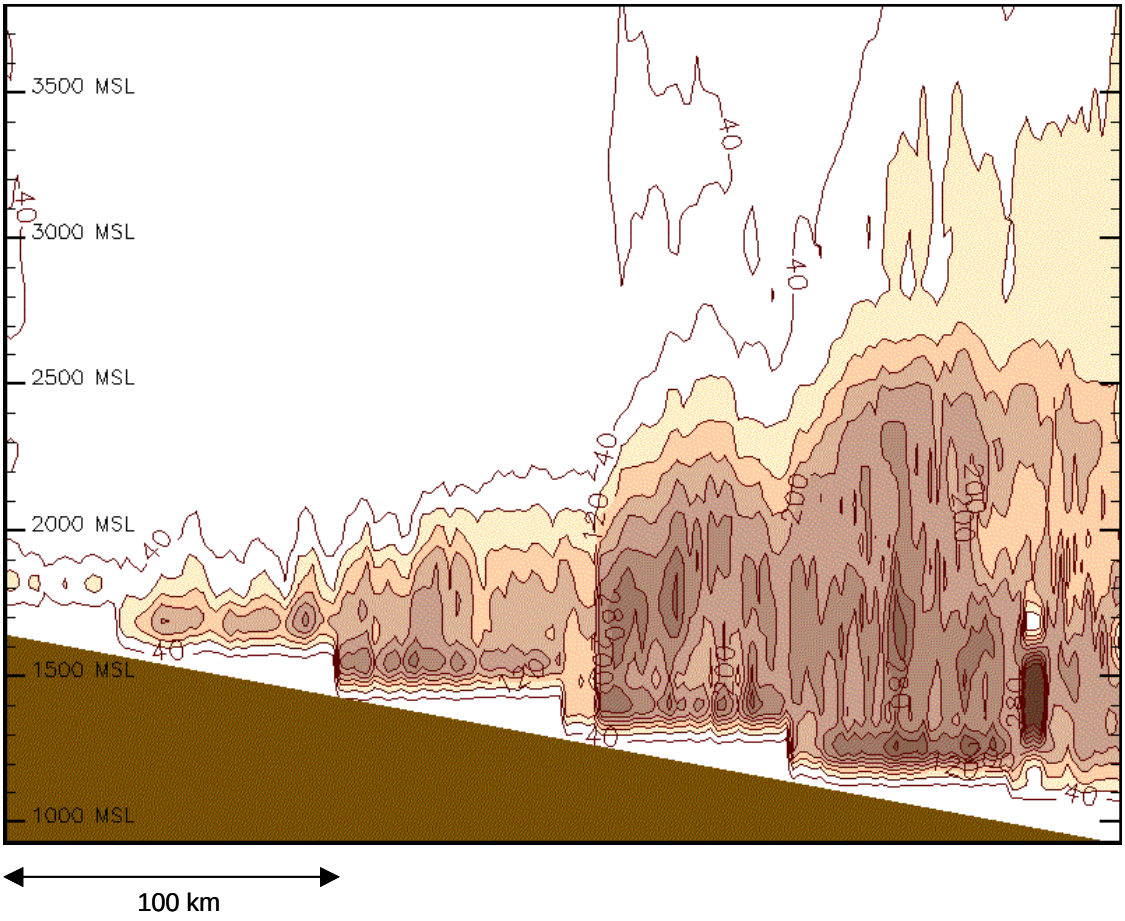

Fig. 6. Lidar-based northward horizontal moisture flux (v x q) orthogonal to a vertical section along the northern leg of the aircraft flight box on 9 June 2002. See Figs. 1 and 2 for orientation and text for instrumentation description. Horizontal distances (in km) along the horizontal axis are estimated from aircraft flight-speed and times. Units are gkg^{-1} ms^{-1}. Near-surface stair-step pattern is a nonphysical effect of data discretization; surface terrain is idealized. Flux contour intervals are 40 gkg^{-1} ms^{-1}.

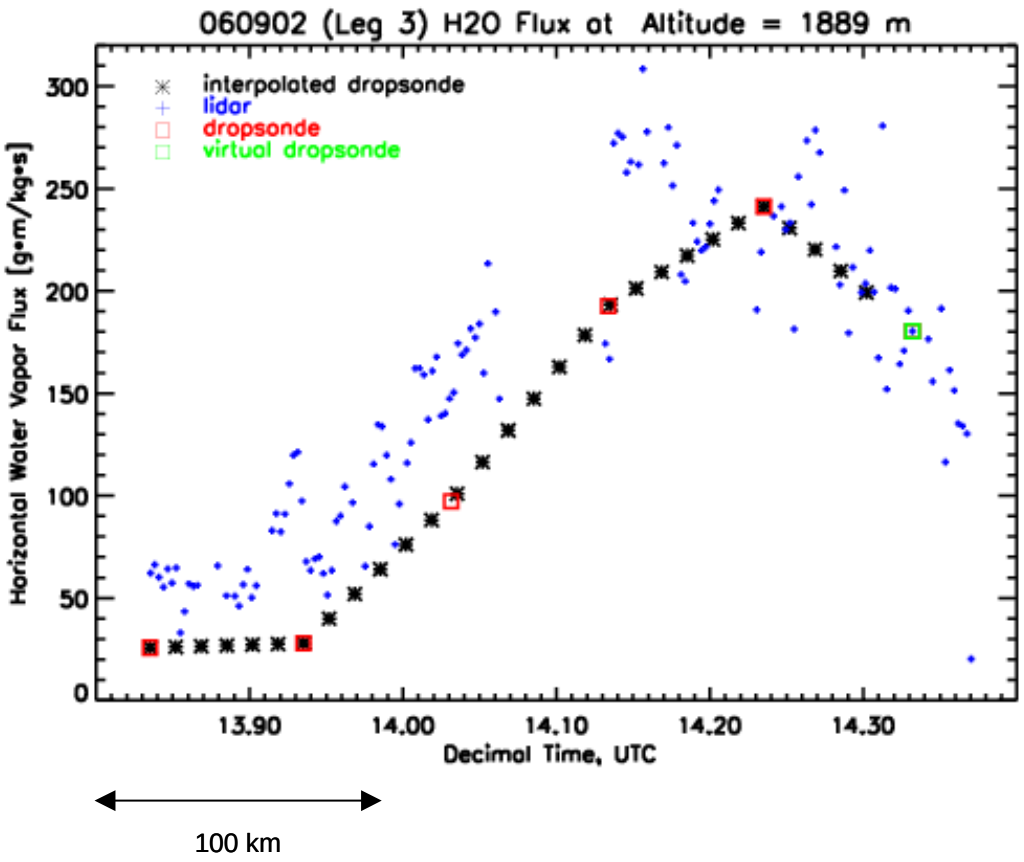

Fig 7. Comparison of lidar-based (blue points) and droposonde-based (red squares and interpolated black x's) northward meridional moisture fluxes along the northern flight leg flown by the DLR Falcon on 9 June 2002.

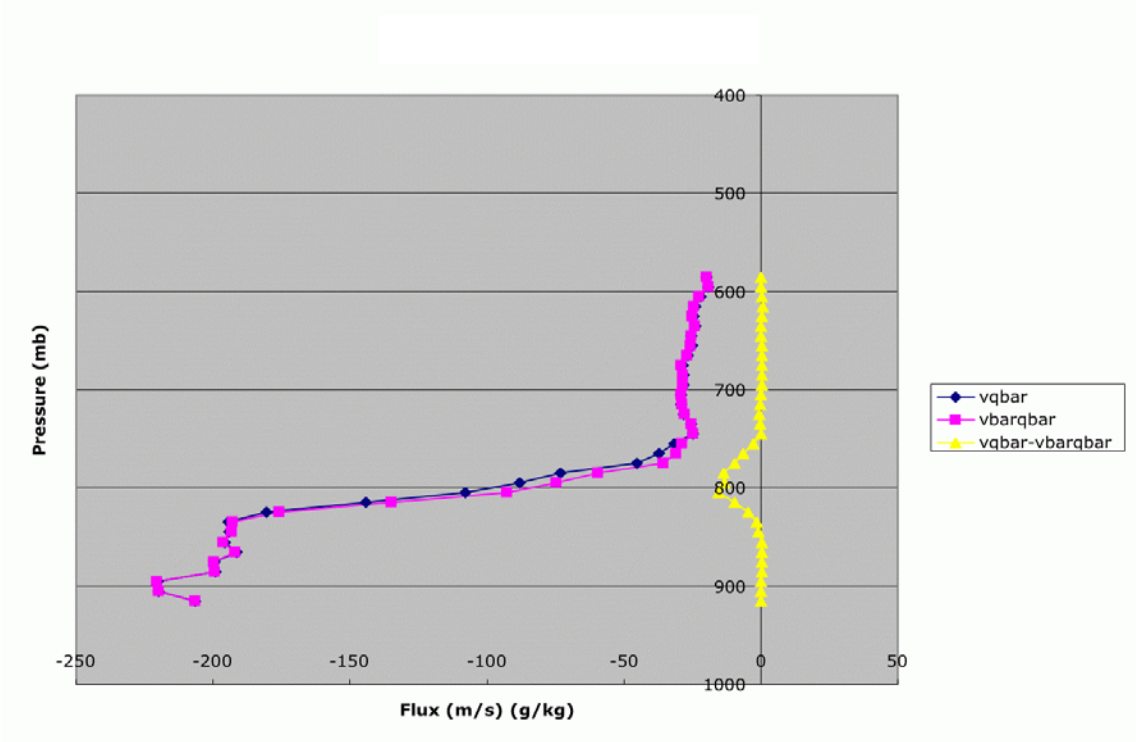

Fig. 8. Components of Reynolds-averaged horizontal moisture flux profiles for the northern flight leg flown by the DLR Falcon on 9 June 2002 between 13:50 and 14:22 UTC. Black diamonds are flux values averaged over dropsonde locations along the flight leg ($\underline{vq}$); lavendar squares are flux values computed by multiplying v and q averaged over dropsonde locations along the flight leg ($\underline{v}\ \underline{q}$); and yellow triangles are differences ($\underline{vq} - \underline{v}\ \underline{q}$), which we interpret as the contribution by unresolved covariances ($\underline{v'q'}$). For reference, the difference minimum near 800 mb corresponds to a height of about 1800 m asl.

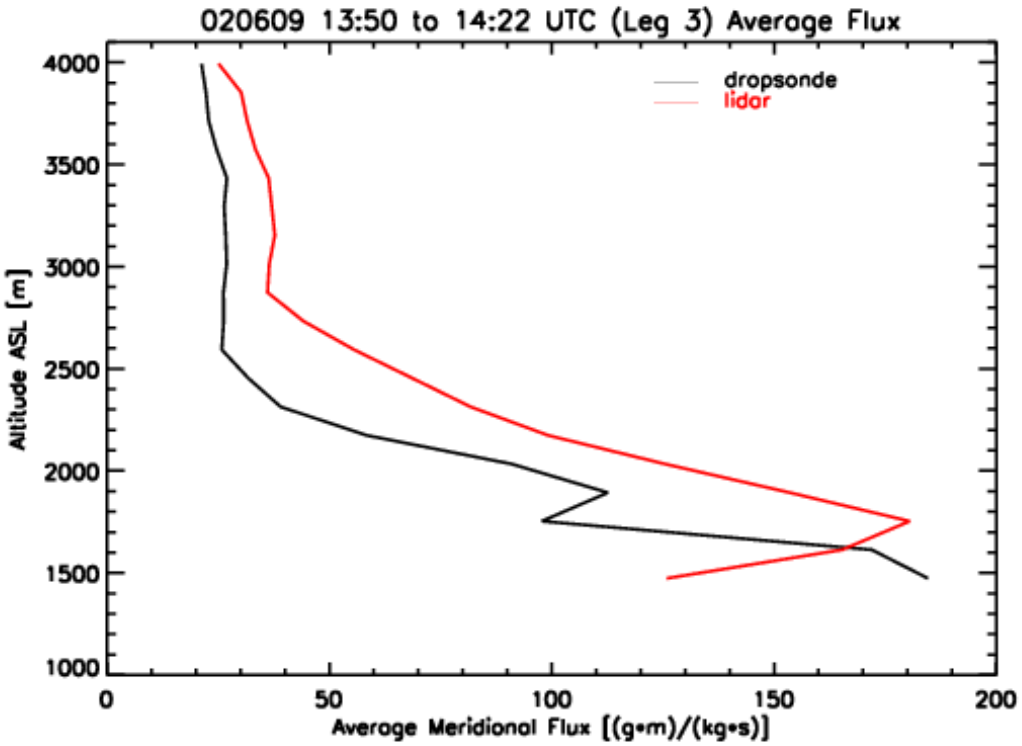

Fig. 9. Flight leg averages of northward meridional moisture flux as computed from dropsonde observations (black curve) and from lidar observations (red curve).

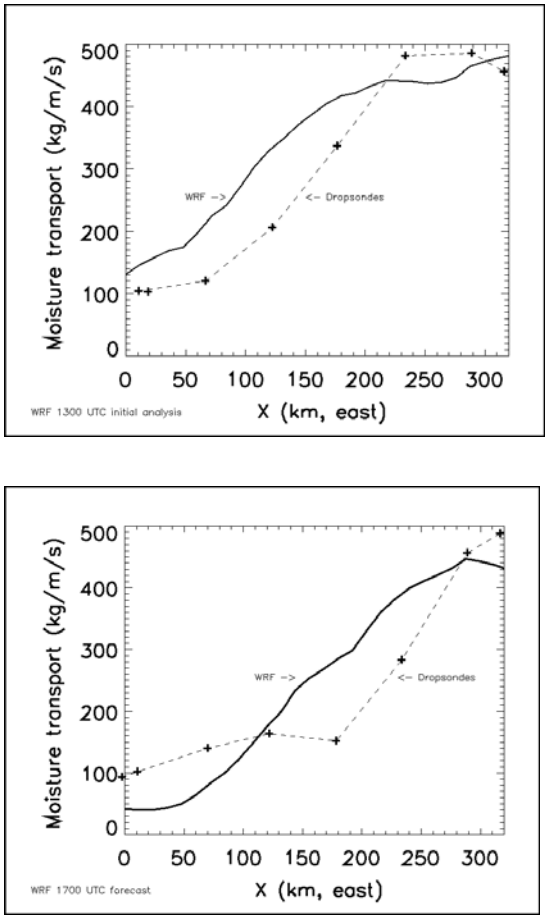

Fig 10. Vertically-integrated density-weighted northward horizontal meridional moisture flux along the north leg of the aircraft flight box as observed by dropsondes (at the locations of the "+" characters) and as computed from WRF model fields. The top panel describes conditions centered at 1300 UTC during the first DLR Falcon circuit. The bottom panel describes conditions centered at 1700 UTC during the second circuit of the Learjet aircraft.